Homogeneous-per-layer patterns in multiplex networks

Busiello, Daniel M.; Carletti, Timoteo; Fanelli, Duccio

Published in:
Europhysics Letters

DOI:
10.1209/0295-5075/121/48006

Publication date:
2018

Document Version
Publisher's PDF, also known as Version of record

A LETTERS JOURNAL EXPLORING THE FRONTIERS OF PHYSICS

OFFPRINT

Homogeneous-per-layer patterns in multiplex networks

DANIEL M. BUSIELLO, TIMOTEO CARLETTI and DUCCIO FANELLI

EPL, **121** (2018) 48006

A Letters Journal Exploring the Frontiers of Physics

AN INVITATION TO SUBMIT YOUR WORK

epljournal.org

The Editorial Board invites you to submit your letters to EPL

EPL is a leading international journal publishing original, innovative Letters in all areas of physics, ranging from condensed matter topics and interdisciplinary research to astrophysics, geophysics, plasma and fusion sciences, including those with application potential.

The high profile of the journal combined with the excellent scientific quality of the articles ensures that EPL is an essential resource for its worldwide audience. EPL offers authors global visibility and a great opportunity to share their work with others across the whole of the physics community.

Run by active scientists, for scientists

EPL is reviewed by scientists for scientists, to serve and support the international scientific community. The Editorial Board is a team of active research scientists with an expert understanding of the needs of both authors and researchers.

OVER
568,000
full text downloads in 2015

18 DAYS
average accept to online publication in 2015

20,300
citations in 2015

"We greatly appreciate the efficient, professional and rapid processing of our paper by your team."

Cong Lin
Shanghai University

Six good reasons to publish with EPL

We want to work with you to gain recognition for your research through worldwide visibility and high citations. As an EPL author, you will benefit from:

1. **Quality** – The 60+ Co-editors, who are experts in their field, oversee the entire peer-review process, from selection of the referees to making all final acceptance decisions.
2. **Convenience** – Easy to access compilations of recent articles in specific narrow fields available on the website.
3. **Speed of processing** – We aim to provide you with a quick and efficient service; the median time from submission to online publication is under 100 days.
4. **High visibility** – Strong promotion and visibility through material available at over 300 events annually, distributed via e-mail, and targeted mailshot newsletters.
5. **International reach** – Over 3200 institutions have access to EPL, enabling your work to be read by your peers in 100 countries.
6. **Open access** – Articles are offered open access for a one-off author payment; green open access on all others with a 12-month embargo.

Details on preparing, submitting and tracking the progress of your manuscript from submission to acceptance are available on the EPL submission website **epletters.net**.

If you would like further information about our author service or EPL in general, please visit **epljournal.org** or e-mail us at **info@epljournal.org**.

EPL is published in partnership with:

European Physical Society | Società Italiana di Fisica | EDP Sciences | IOP Publishing

A Letters Journal Exploring the Frontiers of Physics

February 2018

EPL, **121** (2018) 48006
doi: 10.1209/0295-5075/121/48006

www.epljournal.org

Homogeneous-per-layer patterns in multiplex networks

Daniel M. Busiello[1], Timoteo Carletti[2] and Duccio Fanelli[3]

[1] *Department of Physics and Astronomy "G. Galilei" and INFN, Universitá di Padova - Via Marzolo 8, 35131 Padova, Italy*
[2] *Department of Mathematics and Namur Institute for Complex Systems - naXys, University of Namur rempart de la Vierge 8, B 5000 Namur, Belgium*
[3] *Department of Physics and Astronomy, University of Florence, INFN and CSDC - Via Sansone 1, 50019 Sesto Fiorentino (FI), Italy*

received 26 January 2018; accepted in final form 3 April 2018
published online 20 April 2018

PACS 89.75.Hc – Networks and genealogical trees
PACS 89.75.Kd – Patterns
PACS 89.75.Fb – Structures and organization in complex systems

Abstract – A new class of patterns for multiplex networks is studied, which consists in a collection of different homogeneous states each referred to a distinct layer. The associated stability diagram exhibits a tricritical point, as a function of the inter-layer diffusion coefficients. The patterns, made of alternating homogeneous layers of networks, are dynamically selected via non-homogeneous perturbations superposed to the underlying, globally homogeneous, fixed point and by properly modulating the coupling strength between layers. Furthermore, layer-homogeneous fixed points can turn unstable following a mechanism *à la* Turing, instigated by the intra-layer diffusion. This novel class of solutions enriches the spectrum of dynamical phenomena as displayed within the variegated realm of multiplex science.

Countless systems in Nature exhibit patterns and regularities. Chemistry [1,2], biology [3,4] and neuroscience [5] are just few examples of fields in which a macroscopic order spontaneously emerges from the microscopic interplay between many interacting agents.

A particular subset of processes driving the onset of patterns is represented by reaction-diffusion systems, *i.e.* systems made of at least two interacting species undergoing spatial diffusion. Introduced in the context of mammals pigmentation by Alan Turing [6], these systems obey an activator-inhibitor dynamics. Under suitable conditions, the diffusion drives an instability by amplifying a perturbation superposed to a homogeneous stable fixed point. The perturbation grows and, balanced by non-linear interactions, leads to spatially inhomogeneous steady states, termed in the literature Turing patterns.

Although regular lattices define a suitable framework to model physical reaction-diffusion systems, recently the theory has been extended so as to include complex networks [7], as the underlying medium where species are bound to diffuse. This approach is motivated by the fact that many real-world systems, ranging from ecology [8] to the brain structure [9], passing through the modeling of social communities [10], can be easily schematised by invoking the concept of graph [11]. In this context, numerous works have revealed a plethora of interesting phenomena, ascribing to the discrete nature of the embedding support a leading role [12,13].

However, the standard approach to network theory is not always able to encode for the high complexity of real-world systems, *e.g.*, the human brain [14], the transportation network [15,16] and, in general, systems composed by multiple sub-layers. For this reason, a step forward has been taken in the modeling which led to the introduction of the concept of multiplex networks, *i.e.*, interconnected multi-layered graph [17]. The properties of multiplex networks have been widely addressed in the literature. This includes investigating the non-trivial interplay between structure and dynamics [18–20]. A general theory for Turing patterns on multiplex networks has been developed in [21,22]. Interestingly, diffusion among adjacent layers can enhance or suppress the instability [21].

In this work we analyse further the zoology of phenomena that can emerge from a reaction-diffusion system defined on multiplex networks. In particular, we focus on a new class of instability-driven patterns, veritable attractor of the inspected system, which are homogeneous per layer [23], as depicted in fig. 1. These states can turn

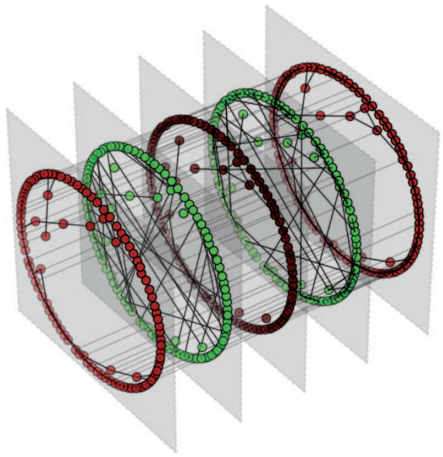

Fig. 1: (Color online) Illustrative example of a layer-homogeneous fixed point as obtained for the case of a multiplex network composed by $M = 5$ Watts-Strogatz layers [24], with probability of rewiring $p = 0.5$ and average connectivity ranging from 2 to 5. Each network is made of $N = 100$ nodes. Here, the Brusselator model is assumed, with parameter $b = 9$, $c = 30$. The diffusion constant are set to the values $D_u^{12} = D_u^{23} = D_u^{34} = D_u^{45} = 1$ and $D_v^{12} = D_v^{23} = D_v^{34} = D_v^{45} = 10$. To facilitate visualization, only 30% of the links in each layer and 40% of the links among layers have been drawn.

unstable due to the injection of a non-homogeneous perturbation which may resonate with the intra-layer diffusion terms. Each layer of a multiplex network can be also thought as an individual node of a corresponding network of layers. In this setting, it is tempting to interpret the novel family of fixed points as coarse-grained patterns, which combines different macro-units so as to reflect the complexity of a multi-layers arrangement. We shall also prove that such coarse-grained patterns can be dynamically selected following a Turing-like instability of the global homogeneous equilibrium, the inter-layer diffusivity acting as the key control parameter.

Let us consider for the sake of simplicity a multiplex composed by two layers, but observe that the model can be readily extended to the case of M-independent layers; each layer is constituted by N nodes, and characterised by a $N \times N$ adjacency matrix A_{ij}^K, where the label $K = 1, 2$ denotes the layer of pertinence. By definition, $A_{ij}^K = 1$ if the nodes i and j are connected in the layer K, $A_{ij}^K = 0$ otherwise. Let us observe that homologous nodes, *i.e.*, the "same node" belonging to different layers, are, by definition, mutually connected. A two-species reaction-diffusion system can hence be cast in the following form [21]:

$$\begin{aligned} \dot{u}_i^K &= f\left(u_i^K, v_i^K\right) + D_u^K \sum_{j=1}^{N} L_{ij}^K u_j^K + D_u^{12}\left(u_i^{K+1} - u_i^K\right), \\ \dot{v}_i^K &= g\left(u_i^K, v_i^K\right) + D_v^K \sum_{j=1}^{N} L_{ij}^K v_j^K + D_v^{12}\left(v_i^{K+1} - v_i^K\right), \end{aligned} \tag{1}$$

assuming $K = 1, 2$ and $K + 1$ to be 1 for $K = 2$. Here u_i^K and v_i^K stand for the concentrations of the species on the node i, as seen in layer K. L_{ij}^K is the Laplacian matrix associated to the K layer, $L_{ij}^K = A_{ij}^K - k_i^K \delta_{ij}$, where $k_i^K = \sum_j A_{ij}^K$ refers to the connectivity of node i belonging to layer K (see footnote [1]) and δ_{ij} is Kroenecker's delta. The matrix L_{ij}^K is nothing but the discrete version of a diffusion operator. D_u^K (respectively, D_v^K) is the intra-layer diffusion coefficient of species u (respectively, v); D_u^{12} (respectively, D_v^{12}) denotes the inter-layer diffusion coefficient associated to species u (respectively, v). Finally, the non-linear functions $f(\cdot, \cdot)$ and $g(\cdot, \cdot)$ encode for the local (on site) rule of interaction between the two considered species. In the following we shall assume that one species acts as an activator, by autocatalytically enhancing its own production, while the other behaves as an inhibitor, contrasting the activator growth.

The model in eq. (1) admits two classes of fixed points: i) the globally homogeneous (GH) fixed points, *i.e.* $u_i^K = \hat{u}$ and $v_i^K = \hat{v}$ for all $i = 1, \ldots, N$ and for all K, namely the equilibrium values are independent of the node and the layer; ii) the layer-homogeneous (LH) fixed points, defined as $u_i^K = \hat{u}^K$ and $v_i^K = \hat{v}^K$ for all $i = 1, \ldots, N$. Note that we here emphasised the dependence of the equilibrium value on the layer, through the index K.

To be concrete, let us consider a specific case study, the so-called Brusselator model for which the local reaction terms are given by $f(u, v) = 1 - (b + 1)u + cu^2 v$ and $g(u, v) = bu - cu^2 v$, depending on the parameters b and c. A straightforward computation allows one to determine the GH fixed point $\hat{u} = 1$, $\hat{v} = b/c$. Determining the LH fixed point proves more demanding and, to this end, we rely on numerical methods. In the following, the parameters of the model are assigned so that the corresponding GH fixed point is stable to external homogeneous perturbation. In other words, (b, c) are selected in the region where the a-spatial version of the Brusselator (*i.e.*, the model obtained when setting to zero all diffusion constants in eqs. (1)) returns a stable fixed point.

Note that the GH fixed point depends only on the model parameters b and c, since both the intra-layer and the inter-layer diffusions vanish when all the nodes share the same concentration, independently of the layer that they are bound to occupy. On the other hand, LH fixed points are also functions of the inter-layer diffusion coefficients, D_u^{12} and D_v^{12}, but do not depend on the intra-layer diffusion constants, because the species display an identical concentration on each layer, at equilibrium. Importantly, the existence of these two classes of fixed points is independent of the underlying topology of the layers composing the multiplex network.

To study the stability of the above-mentioned fixed points, we perform a standard linear stability analysis and monitor the time evolution of a perturbation assumed homogeneous per layer. In formulae, we shall

[1] Notice that k_i^K does not account for inter-layers links.

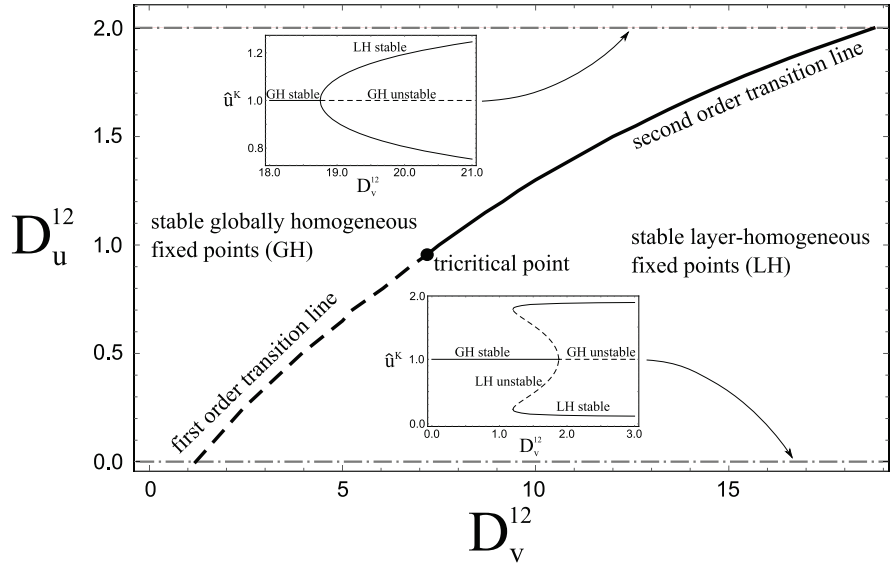

Fig. 2: Main panel: phase transitions in the reference plane (D_u^{12}, D_v^{12}) for a multiplex network composed of two layers. Each layer is made of a Watts-Strogatz network with $N = 100$ nodes, probability of rewiring $p = 0.5$. The upper Watts-Strogatz network originates from a ring with just nearest-neighbors couplings, while for the other network a third nearest-neighbors lattice is assumed, as the initial skeleton. The curves refer to the Brusselator reaction model with $b = 9$ and $c = 30$. The dashed line refers to the first-oder transition, the solid line stands for the second-order transition, the circle identifies the position of the tricritical point. In the lower portion of the plane, LH solutions are stable. Viceversa, in the upper region of the plane, GH fixed points represent the stable equilibria. Upper inset: second-order bifurcation diagram. $\hat{u}^K$ is plotted as a function of D_v^{12}, for $D_u^{12} = 2$ (dash-dotted upper line). GH solutions return an identical value of $\hat{u}^K$, on both layers. GH solutions appear hence as a degenerate single curve. LH fixed points yield two distinct profiles, each associated to one of the layers of the examined multiplex. Lower inset: first-order bifurcation diagram. $\hat{u}^K$ is represented as a function of D_v^{12}, for $D_u^{12} = 0$ (dash-dotted lower line). The qualitative scenario here depicted is robust against modulating the reaction parameters involved (as, *e.g.*, b and c), and/or altering the topology of the employed networks.

set $u_i^K = \bar{u} + \delta u^K$ and $v_i^K = \bar{v} + \delta v^K$, $\forall i$, where $\bar{u}$ (respectively, $\bar{v}$) is either $\hat{u}$ (respectively, $\hat{v}$) or $\hat{u}^K$ (respectively, $\hat{v}^K$), and linearise eqs. (1), for $\delta u^K, \delta v^K$ small. The analysis materialises in an interesting picture, which can be efficaciously summarised in the plane (D_u^{12}, D_v^{12}), as reported in fig. 2. The parameters space is partitioned into two regions: in the lower portion of the plane LH solutions prove linearly stable. In the upper domain GH fixed points are stable equilibria. The two regions are separated by a transition line which we have determined analytically. The dashed line identifies a first-oder transition: by monitoring $\hat{u}^K$, as a function of D_v^{12}, for D_u^{12} frozen to a value that makes the crossing to happen where the transition is predicted discontinuous (horizontal, lower dash-dotted line), one obtains the typical bifurcation diagram as displayed in the lower inset of fig. 2. Conversely, when the transition is continuous (horizontal, upper dash-dotted line) one recovers the usual pitchfork bifurcation, as shown in the upper inset enclosed in fig. 2. First and second transition lines merge together at a tricritical point, the black circle in fig. 2. The bifurcation diagram follows a linear stability analysis. Formally, this implies computing the spectrum of the Jacobian matrix, evaluated at the fixed point. The transition lines correspond to the condition where the largest real part of the computed eigenvalues is found to be identically equal to zero. Since the fixed points belonging to the LH class cannot be expressed in a closed analytical form, the diagonalisation of the Jacobian is performed numerically. The prediction relies hence on analytical techniques, but to finalise the calculation numerical methods are needed. As an important remark, we recall that other families of critical points have been reported in spreading dynamics on multiplex networks [25–27].

Given the above scenario several interesting questions arise. When operating in the region where the LH fixed point is shown to be stable, can one seed a diffusion-driven instability *à la* Turing, triggered by a random non-homogeneous perturbation? And can one obtain the LH (coarse grained or homogeneous per layer) patterns, as following a symmetry breaking instability of a GH stable equilibrium? These are the questions that we set to answer in the following.

Taking inspiration from [21], we introduce a small perturbation $(\delta u_i^K, \delta v_i^K)$ to the fixed point $(\hat{u}^K, \hat{v}^K)$ and linearise eqs. (1) around it:

$$\frac{\mathrm{d}}{\mathrm{d}t}\begin{pmatrix}\delta\mathbf{u}\\ \delta\mathbf{v}\end{pmatrix} = \boldsymbol{\mathcal{J}}\begin{pmatrix}\delta\mathbf{u}\\ \delta\mathbf{v}\end{pmatrix} \tag{2}$$

with

$$\boldsymbol{\mathcal{J}} = \begin{pmatrix}\boldsymbol{f}_u + \boldsymbol{\mathcal{L}}_u + D_u^{12}\boldsymbol{\mathcal{I}} & \boldsymbol{f}_v\\ \boldsymbol{g}_u & \boldsymbol{g}_v + \boldsymbol{\mathcal{L}}_v + D_v^{12}\boldsymbol{\mathcal{I}}\end{pmatrix},$$

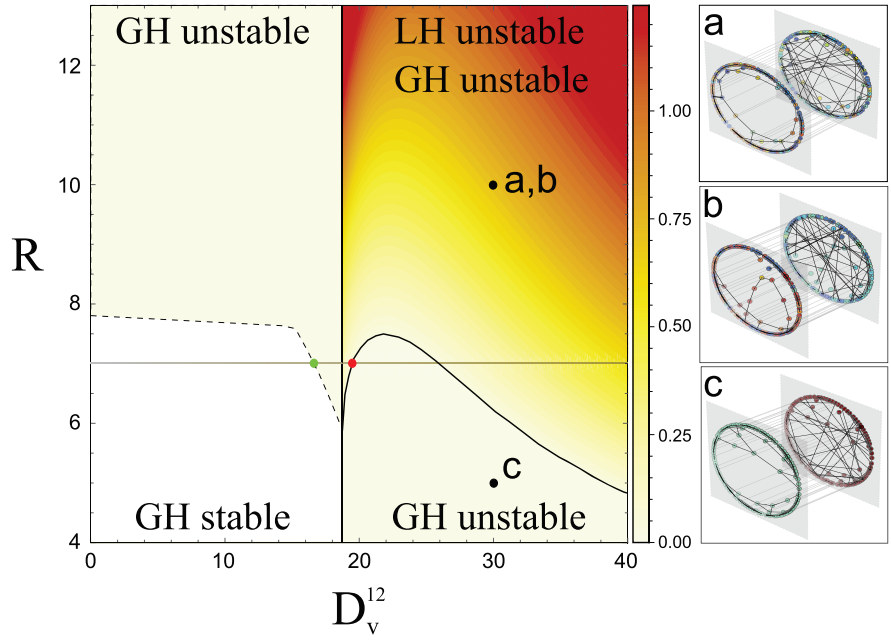

Fig. 3: (Color online) The instability domains associated to GH and LH fixed points are studied in the (D_v^{12}, R)-plane. The Brussellator model is assumed with $b = 9$ and $c = 30$. The inter-layer diffusion coefficient is set to $D_u^{12} = 2$, corresponding to the second-order transition in fig. 2 (similar conclusions can be reached when setting D_u^{12} to a value that yields a first-order transition). The dashed line delineates the upper edge of the GH stability domain (the region of interest is also delimited by the vertical line located at $(D_v^{12})_c$). For $D_v^{12} > (D_v^{12})_c$, the GH is always unstable. Conversely, LH fixed points turn unstable, upon injection of a non-homogeneous perturbation, for a choice of the relevant parameters that position the examined system above the solid line, as obtained via the linear stability analysis. The dispersion relation, calculated as the largest real part of the eigenvalue of $\mathcal{J}$, evaluated at the LH fixed point is plotted, in the region of LH instability, with an appropriate color code. The patterns obtained upon integration of the system are displayed in the inset: (a) and (b) refer to a choice of the parameters where GH and LH are simultaneously unstable (upper black circle in the main panel). Pattern (a) follows a perturbation imposed on the GH equilibrium, pattern (b) assumes LH as the background equilibrium. Coarse-grained patterns can emerge from a GH fixed point, in the region where LH is stable to external perturbation (panel (c)). The networks employed have size $N = 100$. They have been generated by using the Watts-Strogatz recipe [24], with probability of rewiring $p = 0.5$, and assuming a first nearest-neighbors ring as an underlying skeleton for the upper layer, and a third nearest-neighbors lattice for the lower. The (green and red) circles in the main panel stand for the transition points between different regimes, as found when cutting at $R = 7$.

where use has been made of the compact notation $\mathbf{x} = (x_1^1, \dots, x_N^1, x_1^2, \dots, x_N^2)$ for $x = u, v$, and $\mathcal{I} = \begin{pmatrix} -I_N & I_N \\ I_N & -I_N \end{pmatrix}$, with I_N the $N \times N$ identity matrix. The supra Laplacian [28] for species u reads $\mathcal{L}_u = \begin{pmatrix} D_u^1 L^1 & 0 \\ 0 & D_u^2 L^2 \end{pmatrix}$. Analogously, for species v. Moreover, we have introduced the $4N \times 4N$ matrix

$$f_u = \begin{pmatrix} \partial_u f|_{(\hat{u}^1, \hat{v}^1)} I_N & 0 \\ 0 & \partial_u f|_{(\hat{u}^2, \hat{v}^2)} I_N \end{pmatrix}$$

and, similarly for f_v, g_u and g_v. These additions constitute the main difference with respect to the standard Turing theory.

Studying the $4N$ eigenvalues of the matrix $\mathcal{J}$, we can derive the conditions for the dynamical instability which anticipates the onset of the patterns. In fact, if the real part of at least one eigenvalue is positive, the perturbation grows exponentially in the linear regime. Non-linear effects become eventually important: they compensate for the linear growth and consequently shape the final non-homogeneous stationary configuration.

From an analytical point of view [21], one cannot introduce a basis to expand the perturbations which diagonalise the global diffusion operators $\mathcal{L}_u + D_u^{12}\mathcal{I}$ and $\mathcal{L}_v + D_v^{12}\mathcal{I}$. We cannot hence simplify the $4N \times 4N$ eigenvalue problem, by projecting it into a reduced subspace, as it is instead possible when the dynamics is hosted on just one isolated layer [7]. Moreover, the spectrum of $\mathcal{J}$ cannot be exactly related to the spectra of the homologous operators, obtained for the limiting setting when the two layers are formally decoupled ($D_u^{12} = D_v^{12} = 0$).

It is, however, possible to determine numerically the region where the diffusion-driven instability is bound to occur, and then integrate the set of governing differential equations, so as to visualise the ensuing patterns. To this aim, we fix the reaction parameters of the inspected model (b and c, in the case of the Brusselator model), and one of the inter-layer diffusion coefficients, specifically D_u^{12}. When modulating D_v^{12}, at fixed D_u^{12}, one operates an

horizontal cut of fig. 2. According to the usual Turing theory, referred to standard mono-layered graphs, the ratio of species' diffusivities matters and ultimately determines the onset of the instability. In analogy, we here introduce $R^K = D_v^K/D_u^K$, the diffusivities ratio as measured on layer K. In the following, for the sake of simplicity, we will set $R^1 = R^2 = R$, still limiting the analysis to the minimal choice $K = 2$. The parameter R keeps track of the intra-layer diffusion, while the inter-layer diffusion (hence the associated ratio) can be solely adjusted by acting on D_v^{12}. Several regions are identified, when spanning the parameters in the relevant plane (D_v^{12}, R), see main panel of fig. 3. The GH fixed points are stable to external homogeneous perturbations in the (white) region delimited i) from the above by the dashed solid line, and ii) from the right by the vertical solid line located at $(D_v^{12})_c \simeq 18$. In the complementary region of the plane, the GH equilibria get destabilised by injection of a non-homogeneous disturbance, which is then self-consistently amplified. The solid line depicted for $D_v^{12} > (D_v^{12})_c$, identifies the threshold of instability for the LH fixed point, as determined via the above linear stability analysis. In the domain of LH instability (contained within the region of GH instability), the largest real part of the eigenvalues (also called dispersion relation) of $\mathcal{J}$, evaluated at the LH fixed point, is represented with an appropriate color code. Several comments are mandatory at this point. First, LH Turing patterns are instigated by increasing the inter-layer diffusion constant D_v^{12} (or, equivalently, the ratio D_v^{12}/D_u^{12}). Interestingly by tuning D_v^{12} one can drive unstable a system which is otherwise stable, under the classical Turing paradigm applied to GH equilibria, for $D_v^{12} = 0$. Further, two alternative pathways can be pursued for pattern generation, in the region where GH and LH are both unstable. The emerging patterns are annexed as insets (a) and (b) of fig. 3, and display similar qualitative traits. Moreover, a diffusion-driven instability of a GH equilibrium can take the system towards the basin of attraction of a stable LH fixed point, as shown in panel (c) of fig. 3. As anticipated, it is therefore possible to obtain a LH equilibrium as the dynamical outcome of a genuine Turing instability, acting on a GH fixed point. LH equilibria could be hence interpreted as a special class of Turing patterns. Remark that these latter could be radically simplified at the coarse-grained scale, by replacing each layer with a single macro-unit, which bears the very same concentration that happens to be shared by the nodes that define the fine structure of the layer.

The above scenario remains unchanged, when modulating the topological characteristics of the networks associated to the two layers. More precisely, by assuming other topologies for the underlying networks, *e.g.*, heterogeneous connectivities, can quantitatively impact the dispersion relation, the associated bifurcation diagram and the ensuing patterns. The qualitative framework that we have delineated holds however in general, irrespectively of the topological characteristics of the networks to which species happen to be bound. In this respect, it is important to remark again that the LH fixed points are insensitive to the specificity of the networks that compose the multiplex. Similarly, the reaction model can be changed, the Brusselator being just one out of many possible choices, yielding a substantially identical picture (data not shown). The only formal requirement is the existence of a stable homogeneous fixed point, as in the spirit of the Turing analysis.

To discriminate between distinct classes of ensuing patterns we introduce the following indicator:

$$\Gamma = \frac{1}{N}\sum_{i=1}^{N}\Theta(|u_i^1 - u_i^2|) - \frac{1}{4N}\sum_{K=1}^{2}\sum_{i=1}^{N}\Theta\left(\left|\sum_{j=1}^{N} L_{ij}^K u_j^K\right|\right),$$

where $\Theta(\cdot)$ is the Heaviside function. This indicator is simply meant to identify the different patterns that can be attained by the system (in the two layers configuration), as following a symmetry breaking instability, seeded by the injection of an external perturbation. By evaluating Γ at large times, *i.e.*, when the system has eventually reached its asymptotic configuration, one obtains in fact three possible outcomes. When the system is confined in a globally homogeneous fixed point, $\Gamma = 0$, since both contributions entering the above definition vanish identically. On the contrary, if the system exhibits a disordered pattern, the first term is approximately equal to one, because in general $u_i^1 \neq u_i^2$, and the second term is equal to $1/2$, so yielding $\Gamma \simeq 1/2$. Finally, when the system lands in a layer-homogeneous fixed point, *i.e.*, a coarse-grained pattern, $\Gamma = 1$, since the second term vanishes, being all the concentrations in the same layer equal. A similar indicator could be introduced to monitor the degree of large-scale organization of the competing species v.

In fig. 4 we report the value of Γ, as a function of the inter-layer diffusion coefficient D_v^{12}. The emerging patterns, classified in terms of Γ, are obtained by perturbing a GH fixed point, assumed stable in absence of diffusion. The results displayed fig. 4 are computed by processing the patterns recorded via direct numerical integration of eqs. (1), and after averaging over different realizations of dynamics. The results refer $D_u^{12} = 2$ (second-order transition), being the other parameters frozen to the values declared in the caption of fig. 2 (qualitatively similar results are obtained when setting D_u^{12} to a value which corresponds to a first-order transition). By eye inspection, it is immediate to conclude that the system exhibits disordered or coarse-grained (homogeneous per layer) patterns, depending on the value of the coupling strength between layers. The regions where different patterns are found, organise in adjacent blocks, as a function of the control parameter D_v^{12}. More specifically, for modest values of D_v^{12}, standard Turing patterns take place. By increasing D_v^{12}, coarse-grained patterns are instead established. The vertical (green and red) lines are respectively drawn in correspondence of the critical values of D_v^{12}, as identified in fig. 3, see (red and green) circles. These latter

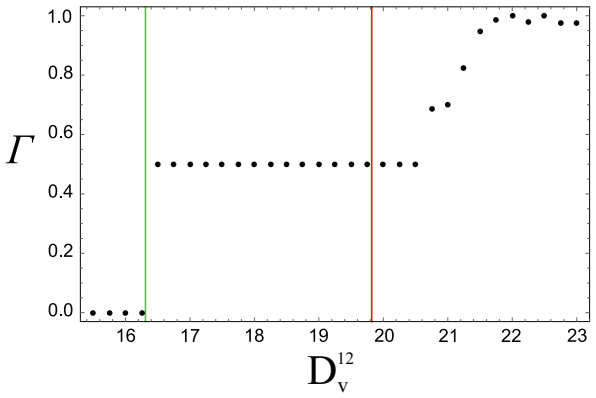

Fig. 4: (Color online) Γ as a function of the inter-layer diffusion coefficient D_v^{12}, as obtained for a Brusselator model with $b = 9$ and $c = 30$. Here, $D_u^{12} = 2$ and $R = 7$ (see horizontal line in fig. 3). The multiplex network is composed of two layers, generated as explained in the caption of fig. 3. Each reported entry refers to averaging over 20 simulations, as the emergence of a LH attractor is a probabilistic event. The green vertical line is traced for a value of D_v^{12} that marks the instability of a GH fixed point, when moving at fixed $R = 7$ (green point in fig. 3). The red vertical line sets the beginning of the region where LH solutions are stable attractors of the dynamics. Representative examples of the obtained patterns are depicted in the insets of fig. 3.

provide a satisfying theoretical interpretation for the observed transitions.

Summing up, we have here developed a theory of pattern formation for a two-species reaction diffusion system on a two-layers multiplex network around a novel class of (layer-homogeneous) fixed points. The methodology can be readily generalised to the case of s interacting species upon K-independent layers. Indeed by allowing for more layers opens up several possibilities. Focus, for example, on the case of three adjacent layers. Three distinct LH fixed points can in principle appear. Alternatively, two networks could share an identical value of the concentration and then bifurcate to yield different homogeneous entries, in correspondence of a (second) bifurcation point, associated to a critical diffusion coefficient (as occurs for the logistic map). Interestingly, the layer-homogeneous fixed points can be seen as coarse-grained patterns in a network of networks where each layer is replaced by a virtual supernode, bearing the concentration displayed by individual micro-nodes, belonging to the layer itself. This novel class of patterns can be dynamically selected by perturbing the globally homogeneous fixed point and assigning the coupling strength between different layers, to fall within a specific window, as we have proven with reference to the two-layers case study. The inter-layer diffusion can promote the onset of patterns formation. This scenario has been tested with reference to the Brusselator model, assumed as a paradigmatic representative, but it holds in general, irrespectively of the specific reaction rules implemented (data not shown). Different kinds of patterns co-exist in systems defined on a stratified network and the diffusion act as trigger to resolve hidden microscopic structures. The potential interest of this observation embraces in principle a large set of applications. For example, ecological networks can be pictured as multi-layered graphs, in which the interactions on each layer influence the dynamics of the whole system [29]. Analogously, the complex topology of the brain can be sometimes represented as a multiplex network [30], the most glaring example being the barrel cortex [31], in which stratified patterns of activity may possibly take place. Exploring the applied relevance of the coarse-grained patterns here discussed remains however a challenge for future investigations.

* * *

The work of TC presents research results of the Belgian Network DYSCO (Dynamical Systems, Control, and Optimization), funded by the Interuniversity Attraction Poles Programme, initiated by the Belgian State, Science Policy Office. The scientific responsibility rests with its author(s). DF acknowledges financial support from H2020-MSCA-ITN-2015 project COSMOS 642563.

REFERENCES

[1] Murray J. D., *Mathematical Biology. II Spatial Models and Biomedical Applications*, *Interdisciplinary Applied Mathematics*, Vol. **18** (Springer-Verlag New York Incorporated) 2001.
[2] Zhabotinsky A. M., Dolnik M. and Epstein I. R., *J. Chem. Phys.*, **103** (1995) 10306.
[3] Suweis S., Simini F., Banavar J. R. and Maritan A., *Nature*, **500** (2013) 449.
[4] Busiello D. M., Suweis S., Hidalgo J. and Maritan A., *Sci. Rep.*, **7** (2017) 12323.
[5] Beggs J. M. and Plenz D., *J. Neurosci.*, **23** (2003) 11167.
[6] Turing A. M., *Philos. Trans. R. Soc. London, Ser. B, Biol. Sci.*, **237** (1952) 37.
[7] Nakao H. and Mikhailov A. S., *Nat. Phys.*, **6** (2010) 544.
[8] May R. M., *Stability and Complexity in Model Ecosystems*, Vol. **6** (Princeton University Press) 2001.
[9] Sporns O., Chialvo D. R., Kaiser M. and Hilgetag C. C., *Trends Cogn. Sci.*, **8** (2004) 418.
[10] Wasserman S. and Faust K., *Social Network Analysis: Methods and Applications*, Vol. **8** (Cambridge University Press) 1994.
[11] Boccaletti S., Latora V., Moreno Y., Chavez M. and Hwang D.-U., *Phys. Rep.*, **424** (2006) 175.
[12] Asllani M., Challenger J. D., Pavone F. S., Sacconi L. and Fanelli D., *Nat. Commun.*, **5** (2014) 4517.
[13] Asllani M., Busiello D. M., Carletti T., Fanelli D. and Planchon G., *Sci. Rep.*, **5** (2015) 12927.
[14] Bullmore E. and Sporns O., *Nat. Rev. Neurosci.*, **10** (2009) 186.
[15] Kurant M. and Thiran P., *Phys. Rev. Lett.*, **96** (2006) 138701.

[16] Zou S.-R., Zhou T., Liu A.-F., Xu X.-L. and He D.-R., *Phys. Lett. A*, **374** (2010) 4406.
[17] Nicosia V., Bianconi G., Latora V. and Barthelemy M., *Phys. Rev. Lett.*, **111** (2013) 058701.
[18] Sole-Ribalta A., de Domenico M., Kouvaris N. E., Diaz-Guilera A., Gomez S. and Arenas A., *Phys. Rev. E*, **88** (2013) 032807.
[19] de Domenico M., Solé-Ribalta A., Cozzo E., Kivelä M., Moreno Y., Porter M. A., Gómez S. and Arenas A., *Phys. Rev. X*, **3** (2013) 041022.
[20] Bianconi G., *Phys. Rev. E*, **87** (2013) 062806.
[21] Asllani M., Busiello D. M., Carletti T., Fanelli D. and Planchon G., *Phys. Rev. E*, **90** (2014) 042814.
[22] Kouvaris N. E., Hata S. and Díaz-Guilera A., *Sci. Rep.*, **5** (2015) 10840.
[23] Tang L., Wu X., Lü J., Lu J.-a. and D'Souza R. M., *Master stability functions for multiplex networks*, arXiv preprint, arXiv:1611.09110 (2016).
[24] Watts D. J. and Strogatz S. H., *Nature*, **393** (1998) 440.
[25] Granell C., Gómez S. and Arenas A., *Phys. Rev. Lett.*, **111** (2013) 128701.
[26] Sanz J., Xia C.-Y., Meloni S. and Moreno Y., *Phys. Rev. X*, **4** (2014) 041005.
[27] De Domenico M., Granell C., Porter M. A. and Arenas A., *Nat. Phys.*, **12** (2016) 901.
[28] Gomez S., Diaz-Guilera A., Gomez-Gardenes J., Perez-Vicente C. J., Moreno Y. and Arenas A., *Phys. Rev. Lett.*, **110** (2013) 028701.
[29] Pilosof S., Porter M. A., Pascual M. and Kéfi S., *Nat. Ecol. Evol.*, **1** (2017) 0101.
[30] De Domenico M., *GigaScience*, **6** (2017) 1.
[31] Petersen C. C., *Neuron*, **56** (2007) 339.